A Spatiotemporal Ontology of Informal Settlements Using a Combination of OBIA–RF With Worldview-3 and Landsat Data

Khlood Ghalibr Alrasheedi, *Fellow, IEEE*, Ashraf Dewan, and Ahmed El-Mowafy, *Member, IEEE*

***Abstract*—An understanding of the spatial distribution of informal settlements within a city is important for urban management decision-making and service infrastructure provision, provides useful information for planners and policymakers, and has a role in minimizing future urban environmental issues. The objective of this article is to evaluate the performance of an ontology of informal settlements mapping for Riyadh city. Satellite data include a combination of medium-resolution Landsat thematic mapper, enhanced thematic mapper plus, and operational land imager, and VHR Worldview-3 imagery. Object-based image analysis (OBIA) technique was employed to identify 30 useful indicators at defined object, settlement, environment, and temporal levels. Time-series analysis (TSA) was undertaken, and a multidimensional model was developed to define the trend of changes through 30 years. The classification process incorporated OBIA, random forest (RF), and LandTrendr techniques. The classification output included delineation of formal and informal settlement boundaries and road networks, as well as vegetated and vacant areas. The final OBIA–RF and TSA classification demonstrated an overall accuracy (OA) of 89% with the corresponding kappa value of 87%. The OBIA–RF classification developed without TSA techniques returned an OA of 87% and kappa value of 84%. The article indicated that using OBIA and RF methods, in combination with LandTrendr, can be a useful tool for planners and decision-makers to identify changes in the land cover of informal settlements within Riyadh city and beyond.**

***Index Terms*—Expert knowledge (EK), informal settlements, Landsat, LandTrendr, object-based image analysis–random forest (OBIA–RF), time-series analysis (TSA), worldview-3.**

I. Introduction

MANY cities, particularly those found in developing countries, have experienced a rise in the growth of informal settlements as the urban areas have expanded [1]. These are usually characterized by low-income communities, have housing issues, and typically suboptimal infrastructure, roads, and other services [2], [3]. Understanding the unique traits of these informal settlements, also known as unplanned areas, is essential when crafting and implementing urban policies. The absence of a universally agreed-upon definition of an informal settlement, however, makes comparisons difficult [4]. These areas can usually be identified based on their physical attributes and socioeconomic characteristics, including high population/housing densities and limited social services [2], [5], [6], [7]. Informal settlements within the Kingdom of Saudi Arabia (KSA) are unique in having medium population densities compared to other parts of the world, which tend to have high population densities. The KSA settlement areas also typically have good road networks and adequate access to public services. They are predominantly situated in or around city centers [8], [9], and exhibit a mixture of very old and new structures. They differ from slum areas in India or Indonesia in that they develop concurrently with newer urban spaces.

Satellite imagery is useful for studying the dynamics of informal settlements by providing data characterized by both high spatial detail and temporal frequency [10], [11], [12], [13]. Techniques based on remote sensing and aerial imagery analysis are proving invaluable for producing maps and spatial information about informal settlements without the need for in situ observations [14]. The medium-resolution imagery provided by Landsat—with a data record spanning over four decades—is one example of this data availability. These tools provide urban policymakers with a synoptic overview of urban layouts [12], [15] as well as evidence of city spatiotemporal dynamics [16], [17].

Kuffer et al. [6] defined three core aspects in the settlement mapping process. The "Where" refers to the location of informal settlements within specific urban areas [9], [18], [19], [20]. The "What" focuses on identifying changes in these informal settlement areas. The "When" focuses on changes taking place over time and the temporal changes [7], [21], [22].

Recent availability of commercial VHR satellite imagery (with submeter accuracy) has led to researchers concentrating more on object analysis than actually monitoring spatiotemporal change [23]. A lack of information regarding the specific spatial and temporal dimensions of informal settlements can, as a result, be a barrier to understanding the actual development dynamics in these areas [24], [25]. This is because research focus timelines are usually for a year or a number of years at most, rather than decades [24], [25]. The complexity inherent in informal settlement characteristics (orientation, material types, building

Received 15 February 2024; revised 30 June 2024; accepted 19 August 2024. Date of publication 28 August 2024; date of current version 18 September 2024. *(Corresponding author: Khlood Ghalibr Alrasheedi.)*

The authors are with the School of Earth and Planetary Sciences, Spatial Sciences Discipline, Curtin University, Perth, WA 6102, Australia (e-mail: k.alrasheedi@postgrad.curtin.edu.au; a.dewan@curtin.edu.au; a.el-mowafy@curtin.edu.au).

Digital Object Identifier 10.1109/JSTARS.2024.3450844

density, narrow streets, and building textures) also provide challenges for longer term temporal studies [7].

Current change detection techniques include but not limited to spectral mixture analysis [26], structural feature analysis [27], fuzzy sets [28], and chi-square transformations [29]. Some challenges arise when using these methods, including spatial heterogeneity issues, the presence of mixed pixels, and assumptions related to linear spectral mixing. To address these issues, a number of more advanced techniques have been developed. This includes object-based image analysis (OBIA) [7], texture analysis [11], [30], and machine learning (ML) [31]. The OBIA technique has been the most commonly used informal settlement detection method in the past two decades [7]. Despite drawbacks, such as low accuracy, and the normal difficulty encountered in using large datasets [9]. The use of ML algorithms, which overcome some of the issues inherent in the above techniques, is now prevalent, and a combination of OBIA and ML techniques [random forest (RF) or support vector machines] is now used for studies on urban areas, agriculture, land surface temperature, biodiversity, ecotourism, and land use and land cover [32].

Alrasheedi et al. [8] and [9] developed a local ontological framework for mapping informal settlements in Riyadh by defining it at the environment, object, and settlement levels. This framework also incorporated indicators suggested by local area experts, and employed OBIA using extremely high-resolution imagery as the data source. These studies were extended by including RF and SVM methods in the initial OBIA. The article concluded that using an OBIA–RF for mapping informal settlements was more effective than using OBIA–SVM [8]. The RF algorithm is a robust choice for diverse remote-sensing classification tasks using a range of data sources [31], [32], (Matarira et al. 2022). OBIA–RF has proven its ability to generate very accurate maps of informal settlement areas. Previous articles have shown that input feature selection is critical in the classification process and directly influences classification accuracy [9], [20], [31], [32]. It should be noted that the effectiveness of the ontological framework and research methodology developed by Alrasheedi et al. [9] for informal settlement mapping has yet to be rigorously tested. This would involve assessing ease of transferability to different locations and the ability to handle diverse datasets. Addressing the intricate challenge of achieving homogeneity within informal settlements and understanding their dynamic expansion trajectories is both important and challenging [33]. It is notable that integration of time-series analysis (TSA) into this methodology can be an avenue that has also not been thoroughly assessed.

This article aims to analyze and validate the performance of a proposed ontology for mapping informal settlements. The process employs multidate Landsat images and Worldview-3 VHR, and expert knowledge (EK) about the local area. Using the advice of these specialists, data extracted from remotely sensed images are used to define 30 suitable indicators at the object, settlement, environ, and temporal levels. The article also aims to address existing gaps in current informal settlement spatiotemporal change monitoring within Riyadh. It will map the changes detected every 5 years for the period 1990–2020. It will then use the previously defined indicators and OBIA–RF to improve the classification process for these changes. Last, it will quantify how successful the use of combined OBIA–RF and TSA techniques has been for mapping informal settlements.

II. Materials and Methods

A. Description of the Study Area

Riyadh, the capital and largest city of the KSA, is located on the Najid Plateau about 600-m above sea level at a latitude of 24°18″ to 25°11″ N and a longitude of 46°15″ to 47°19″ E). The city has undergone rapid urbanization since the 1970s. The population of the city is currently 8 million [8].

Significant investments have been made within the city in areas, such as education, finance, health, and security. The economic expansion and accompanying infrastructural modernization, along with the availability of more affordable accommodation, have been key drivers in people moving from other parts of the region to Riyadh in search of better-paying jobs and a more satisfying lifestyle [9], [34]. The number of informal settlements found in Riyadh is low in comparison to other cities in the KSA. Twenty-seven informal settlement neighborhoods (typically older residential areas), totaling 30.56 km^2, were selected for this study. The final selection was based on the advice of local urban experts. The study area is shown in Fig. 1 and details of the selected neighborhoods are shown in Table I.

B. Data

This article used VHR Worldview-3 and Landsat medium-resolution (30 m) imageries. The VHR image was acquired on 8 June 2021, with a panchromatic resolution of 0.3 m and multispectral resolution of 1.4 m. These data were also used in previous articles [8], [9]. Landsat imagery consisted of 30 years with 0% cloud cover and include thematic mapper (TM) and enhanced thematic mapper plus (ETM+) sensors (1991 to 2020) for the annual period, 1 February–29 February (path 170/row 45). The products were processed at Level-2 (Table II) and strip lines was atmospherically corrected using Gap tool in Envi 5.6 software. The bands used were 1, 2, 3, and 4 (blue, green, red, and infrared) in Landsat 5 TM and 7 ETM+ and 2, 3, 4, and 5 in Landsat 8 operational land imager (OLI; blue, green, red and infrared). Band 1 in Landsat OLI was removed as it has a different spectral reflectance to earlier Landsat series. Thirty annual composites were processed.

C. Ontological Framework

A local ontology of informal settlements of Riyadh was adopted for this article. This used the original 16 indicators recommended by Alrasheedi et al. [9] and adding another 15 new indicators based on EK (Table III). The original digital surface model indicator was removed due to a lack of data for the entire study area. A total of 30 indicators have been used in the current classification process. OBIA parameterization was employed to transform qualitative data into quantitative indicators.

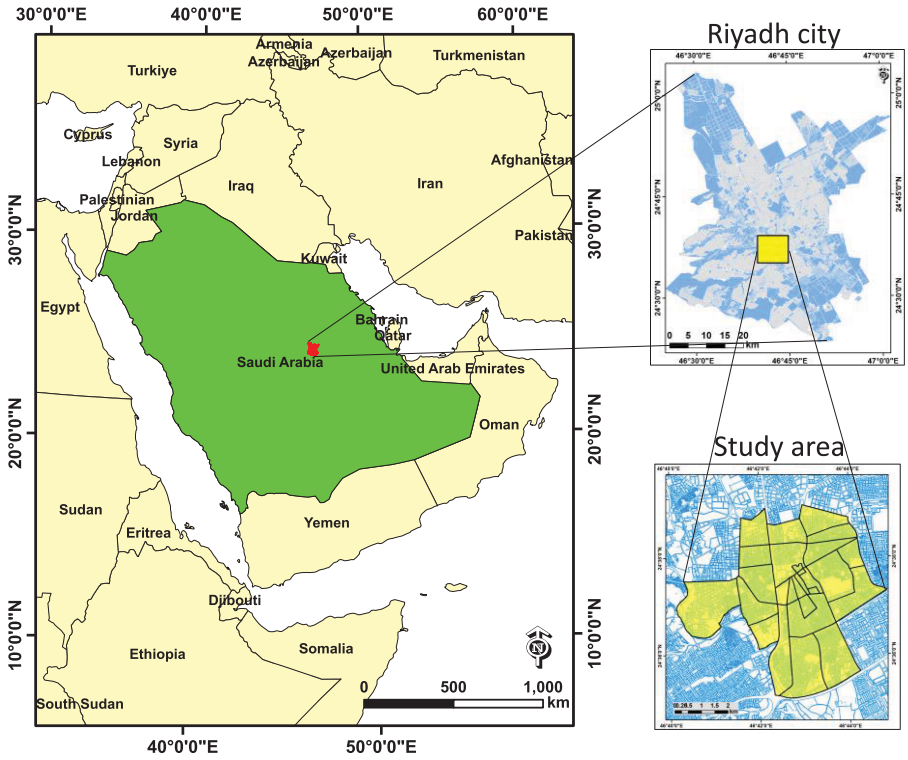

Fig. 1. Location of study areas.

The method used indicators suggested by local EK which utilized to this framework. A temporal level also used to detect informal and formal settlements changes. The associated indicators were included and described using TSA. Thirty Landsat TM, ETM+, and OLI satellite images were used in TSA process. Worldview-3 image was combined with TSA and used for OBIA–RF classification. The workflow employed to map and describe informal settlements is shown in Fig. 2. There are three key steps, they are TSA, OBIA, and OBIA–RF classification.

D. Time-Series Analysis (TSA)

The processing and analysis phase utilized OBIA–RF, LandTrendr, and 30 years of Landsat data. The smallest contribution to the model was made by using TSA with LandTrendr as input data in an ML classifier. The overall accuracy (OA) was achieved for each predicted class. As LandTrendr is a pixel-based algorithm, results should be generalized to mix it with segments to extract the indicators from WorldView-3 imagery.

Thirty Landsat TM, ETM+, and OLI satellite images from 1991 to 2020 were processed to create a multidimensional raster dataset cube representing the Landsat time series. The imagery values were then converted into surface reflectance values. Spectral indices were converted to network common data format to allow easier detection of object changes. The near-infrared (NIR) band (Band 7) provides very good land cover classification information, so this was used during the processing. Spatial and temporal changes in informal and formal settlement areas were flagged using the LandTrendr algorithm which identified key turning points (trend of changes in pixel) within infrared band. The ultimate change trajectory consisted of a series of interconnected linear segments, with the combination of temporal and spectral data at the endpoints of these linear segments to identify the disturbance in informal settlements years by selecting sample points to monitor where the changes were detected. This provided valuable evidence of settlement change.

Time-series turning point changes were identified and used in a comparative analysis of the annual changes visible in the study area. The recovery rate of pixels in a specific year was determined through the subtraction of the recovery values from the preceding year. The algorithm effectively detects land disturbances by analyzing the spatial trends of change in land-cover magnitude (spectral difference), as well as considering the year of disturbance and the duration of these changes. Three raster maps were produced to illustrate the temporal aspects of disturbance and recovery. This included the specific year in which an event occurred, the duration of time of occurrence, and the degree of intensity associated with the change.

E. Image Segmentation and Analysis

1) OBIA Segmentation: Image segmentation was conducted using eCognition software (v 9.2). The segmentation of Landsat and Worldview-3 imagery was achieved using a multiresolution technique. A scale parameter, weighting of shape, and spectral reflectance compactness were defined the during image processing to prevent object overlap [9]. An SP of 30 was selected

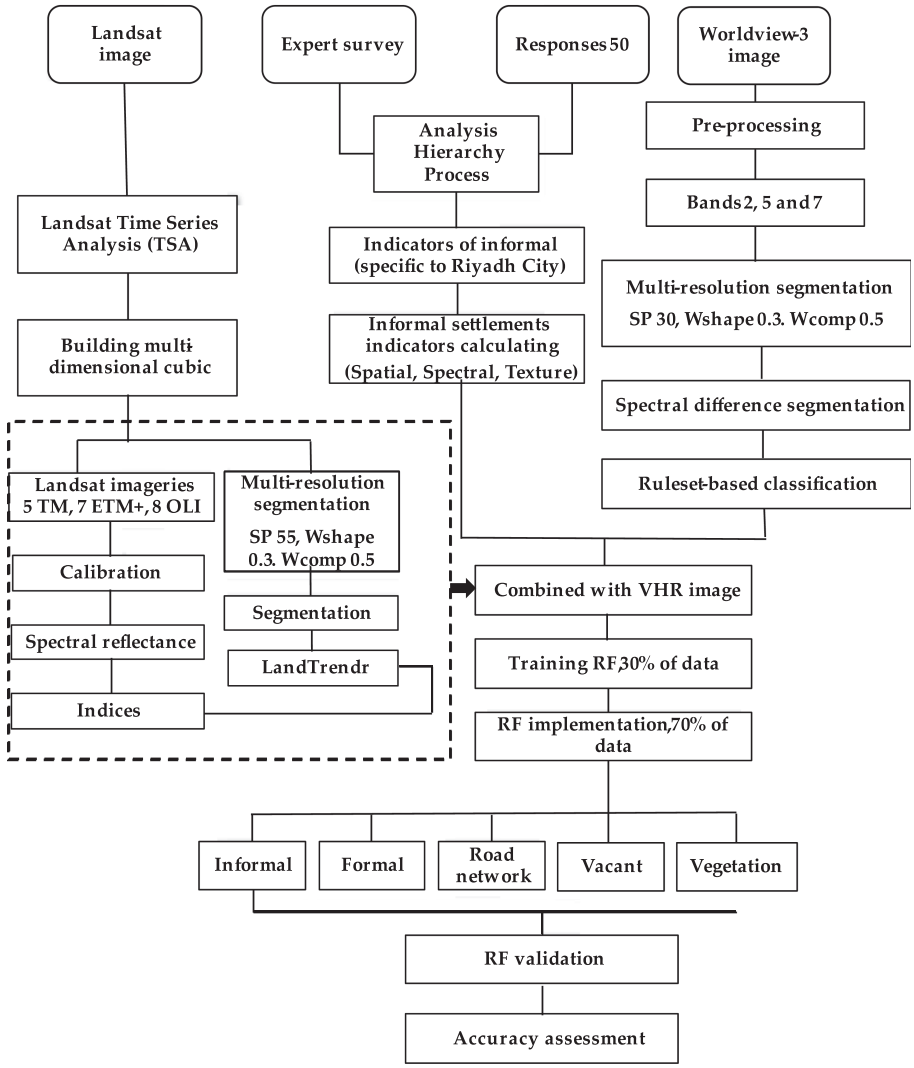

Fig. 2. Workflow, showing methods of this article.

for the Worldview-3 images, and an SP of 55 was selected for the Landsat images. Weighting values of 0.3 and 0.5 were assigned to shape and spectral compactness, respectively. The grey-level cooccurrence matrix (GLCM) was utilized to extract texture from the roof and building. We used five different textural measures: 1) GLCM entropy; 2) GLCM homogeneity; 3) GLCM contrast; 4) GLCM correlation; and 5) GLCM mean. GLCM entropy was used to obtain the building roofs from Band 5 of the Worldview-3 image.

GLCM contrast, GLCM correlation, and GLCMmean measurements were employed to determine lacunarity of housing. This enabled more accurate classification of the various settlement types. Vegetation was extracted using normalized difference vegetation index (NDVI). Thirty indicators were segmented and converted to vectors for input into the OBIA–RF classification process.

2) OBIA–RF Classification: The objects were classified into five classes—informal and formal settlements, road networks, vegetation extent, and vacant land. Thirty indicators were used in the classification. The three raster files produced using LandTrendr (year of change, duration, and magnitude) were combined, and then used as explanatory indicator rasters for training and prediction. The other 27 indicators produced using the OBIA imagery segmentation process were also used for training. The classification operation ran twice: the first time with the TSA features included and then without these features.

F. Training Data

A random sample of 6000 points was created for training purposes, with each point converted into a 2-m radius polygon. Reference samples were randomly selected for use in the training, testing, and validation phases. A total of 30% of the dataset was used for training, and the remaining 70% for implementing the image classification [30], [35]. A total of 500 trees with 30 roots for each tree were used as input for OBIA–RF training. In the training phase, each tree was divided using a bootstrap-aggregating method (bagging) [36]. Ten iterative classification trials were conducted. This guaranteed an accurate estimation of the classifier performance, improved the classifier stability,

TABLE I
SUMMARY OF THE SELECTED NEIGHBORHOODS

Number	Neighboorhood name	Area (km^2)
1	Ad-Dahou	0.081
2	Al-Amal	1.259
3	Aluood	2.116
4	Badeah	3.690
5	Butaha	0.083
6	Derah	1.576
7	Dubeah	0.248
8	Etaigah	1.896
9	Futah	1.115
10	Gubaira	1.751
11	Jaradeah	1.331
12	Jubrah	0.347
13	Manfuha	2.459
14	Margab	0.895
15	Meekal	0.203
16	New Manfuha	1.915
17	Qrai	0.044
18	Salam	0.363
19	Saleheah	0.679
20	Seah	0.951
21	Shemase	1.473
22	Skirinah	0.335
23	Thulaim	0.830
24	Um Sulaem	0.916
25	Wesata	0.140
26	Wesham	1.168
27	Yamamah	2.692
Total area		**30.56**

and accounted for any potential variance in accuracy levels that could occur due to random nature of training sample selection.

G. Accuracy Assessment

The accuracy of the final OBIA–RF classification for each class was determined. Every class type in the image was assessed to make sure the sampled polygons were valid. OA, kappa coefficient (k), and F1-score were generated for accuracy assessment. During RF processing, a random input variable is selected and altered while the remaining variables remain constant. A Gini index is then used to evaluate the decrease in impurity. Classification accuracy was evaluated using out-of-bag (OOB) sample statistics [9]. The current article used a relatively large value (1266) to illustrate the fluctuation in OOB error [8], [30]. Two important parameters, ntree (the number of trees) and mtry (the degree of randomness), were used to determine the effectiveness of the OBIA–RF process [35]. This enabled an accurate assessment of ntree to be considered [30]. The difference between the average of all variables and the variable-specific average was used to determine the significance of each spectral variable in the change detection process. A greater difference indicated a higher level of importance for a given variable. A relative relevance graph was created to rank the relative importance of the parameters (Fig. 9).

III. RESULTS

The multidimensional cube of TSA spatiotemporal difference of informal settlements from 1991 to 2020 is displayed in Fig. 3. An increase and decrease of area in km^2 in informal and formal settlements from 1991 to 2020 is displayed in Fig. 3. Temporal change values (km^2) and (%) for urban settlements between 1991 and 2020 are displayed in Figs. 4 and 5. Fig. 6 shows results of LandTrendr process, 6a is the years of change, 6b is magnitude, and 6c is the duration. Figs. 7 and 8 illustrate the temporal TSA trendline trajectory of informal and formal settlement. Fig. 9 illustrates the relative importance of the 30 indicators. The OBIA–RF classified combination of Worldview-3 and Landsat imagery is shown in Fig. 10. The OA and F1-score of the classification process is defined in Tables IV and V.

A. Change Detection

The classified, multidimension Landsat imagery cube illustrates the spatial and temporal changes in the formal and informal settlement categories—road, vacant area, and vegetation. The periods of individual assessment are 1991–1995, 1995–2000, 2000–2005, 2005–2010, 2010–2015, and 2015–2020 [Fig. 11(a)–(g)]. Each of the periods show significant changes in the above class categories (Fig. 11). The development of informal settlement areas commenced earlier than those for formal settlements and were generally concentrated in the central and southern areas of the city (Fig. 11). Expansion of formal settlements around these initial informal areas is primarily due to the very flat nature of the city terrain. The observed spatial pattern was mainly influenced by ongoing economic development and associated increases in population and services accessibility.

A decrease in the areal extent of informal settlements appears to be associated with ongoing urbanization and government efforts to redevelop the original informal settlement areas into more formal settlements. The amount of settlement area classified as informal in 1991 was calculated to be 27.3 km^2. By 2020, this had decreased to 11.5 km^2. During this same period, the amount of settlement area classified as formal increased from 5.8 to 31.35 km^2 (Fig. 3).

The change in land cover from 1991 to 2020 is shown in Fig. 4. The greatest change in formal settlement areas was between 2005 and 2010, with an increase of 8.54 km^2. Settlement areas identified as informal decreased by 8.16.35 km^2 from 1991 to 2020, with the greatest change noted from 1995 to 2000 (a decrease of 8.79 km^2). From 2000 to 2005, there was not much change noted in informal settlements areas, and these areas decreased to 15.08 km^2 in 2005. Informal settlement area decreased by only 1.33 km^2. There was no significant decrease in the amount of informal settlement area noted from 2005 to 2020 (Fig. 4). The area decreased from 15.12 to 12 km^2 in 2010, 11.46 km^2 in 2015, and finally to 10.77 km^2 in 2020. Vacant areas also decreased during the same period. Otherwise, formal settlements and areas was increased with time as can be seen in Fig. 4.

During the period 1991 to 1995, formal settlements, informal settlements, and vegetation increased by 48%, 9%, and 8%, respectively. From 1995 to 2000, the percentage of formal

TABLE II
CHARACTERISTICS OF SATELLITE IMAGES

Data	Image attributes	Band	Spectral resolution	Ground sampling distance (GSD)	Source
Worldview-3	Panchromatic Band	Panchromatic	450 - 800 nm	0.30 m GSD at nadir 0.34 m at 20° off-nadir	KACST
	MS (multispectral) bands and VNIR (visible near infrared)	Coastal Blue	400 - 450 nm	1.24 m at nadir, 1.38 m at 20° off-nadir	
		Blue	450 - 510 nm		
		Green	510 - 580 nm		
		Yellow	585 - 625 nm		
		Red	630 - 690 nm		
		Red edge	705 - 745 nm		
		Near-infrared1	770 - 895 nm		
		Near-infrared2	400 - 450 nm		
	Acquisition date	8/6/2021			
	Swath width	13.1 km			
	Total cloud cover	0%			
Landsat 5 TM Landsat 7 ETM+	Panchromatic	Panchromatic	510 – 900 nm	15 m GSD	USGS
	MS and NIR	blue	450-520 nm	30 m GSD	
		green	520-600 nm		
		red	630-690 nm		
		Near-infrared	770-900 nm		
		Short-wave infrared	1.55-1.75 nm		
		Short-wave infrared	2.08-2.35 nm		
	Acquis. date	February from 1991-2012			
	Swath width	185 km			
	Total cloud cover	0%			
Landsat 8 OLI	Panchromatic	Panchromatic	500 – 680 nm	15 m GSD	USGS
	MS and NIR	Ultra blue	430-450 nm	30 m GSD	
		blue	450-510 nm		
		green	530-590 nm		
		red	640-670 nm		
		Near-infrared	850-880 nm		
		Short-wave infrared (1)	2.11-2.29 nm		
		Short-wave infrared (2)	450-520 nm		
		Cirrus	1.36-1.38		
	Acquis. date	February from 2013-2020			
	Swath width	180 km			
	Total cloud cover	0%			

TABLE III
ADDITIONAL 15 INDICATORS USED IN THIS ARTICLE

Indicators	Description	Definition
M (G)	Mean green band	Mean brightness in band 3
M (R)	Mean red band	Mean brightness in band 5
M (IR)	Mean infrared band	Mean brightness in band 7
SD (G)	Standard deviation of green band	Dispersion of data in relation to mean brightness in band 3
SD (R)	Standard deviation of red band	Dispersion of data in relation to mean brightness in band 5
SD (IR)	Standard deviation of infrared band	Dispersion of data in relation to mean brightness in band 7
Duration	Spectral difference of duration	The total informal settlements change from 1991 to the 2020
Years of change	Spectral difference of years of change	The periods of temporal change in years
Magnitude	Spectral difference of magnitude	The greatest change of informal settlements
Asymmetry	Housing orientation	Uniformity of housing orientation
Roundness	Similarity of objects	Similarity of an image object to an ellipse
Compactness	Compact of object	The area ratio of object to the circle area with the same perimeter ranged [0 –1]
Border length	Object edges	The sum of edges of the image object shared with surrounding image objects
Rectangular fit	Spatial and geometric of buildings	object consistency into a rectangle of similar size and proportions
Main direction	The eigenvector of the greater of the two eigenvalues	The covariance matrix of the spatial distribution of the image object

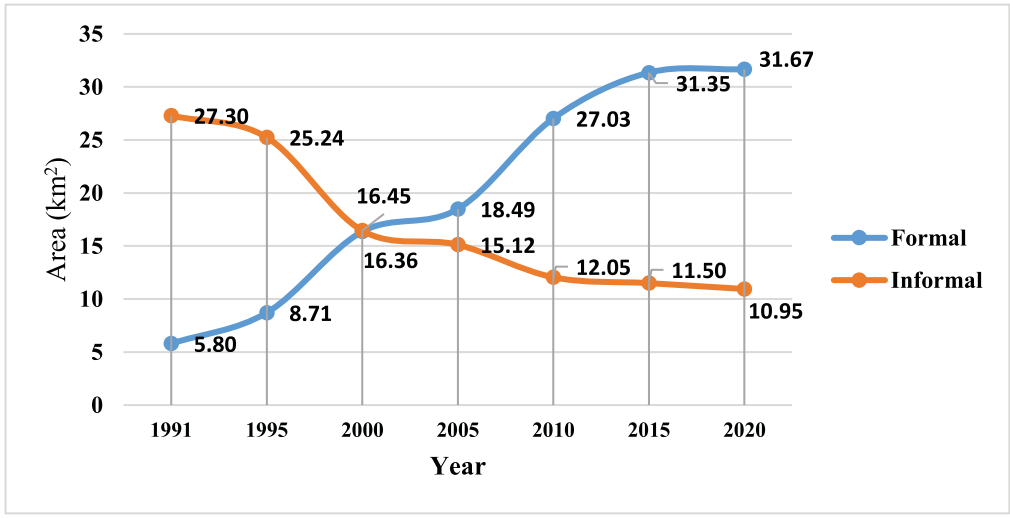

Fig. 3. Relative change in total informal and formal settlement areas (km^2)—1991 to 2020.

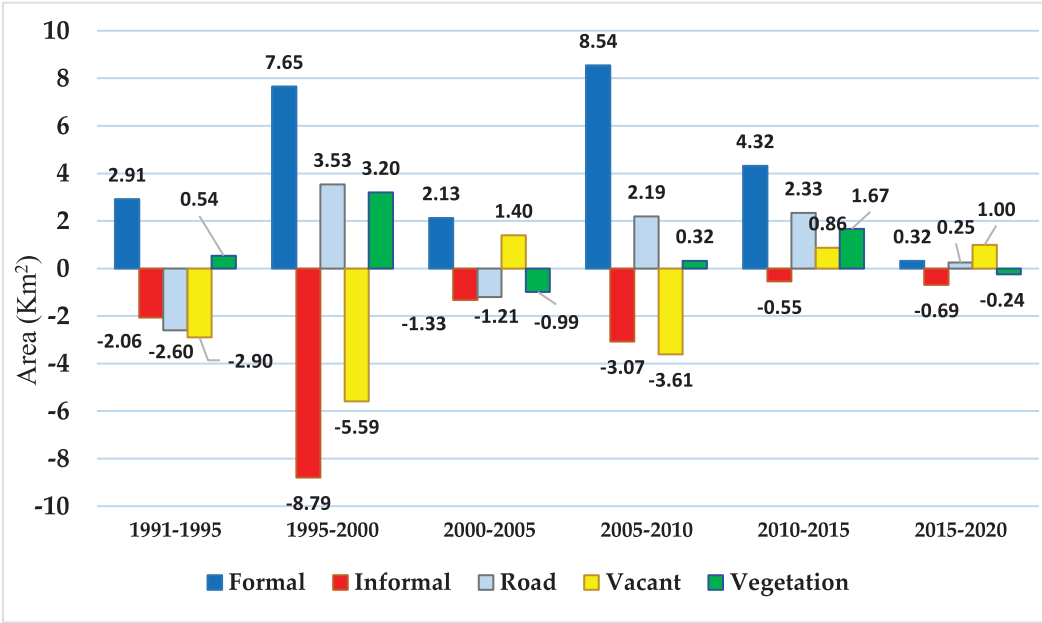

Fig. 4. Changes in land cover areas (km^2)—1991 to 2020.

settlements, roads, and vegetation increased by 87%, 64%, and 45%, respectively. During this period, the percentage of informal settlements and vacant area decreased by 35% and 40%, respectively. This indicates an increase in planned construction. From 2000 to 2005, formal settlement areas and vacant areas increased by 13% and 17%, respectively, and informal settlements, roads, and vegetated areas decreased by 8%, 11%, and 10%, respectively (Fig. 5).

These results indicate removal of informal settlements and replacement with formal settlements. From 2005 to 2010, formal settlements, roads, and vegetation increased by 46%, 22%, and 3%, while informal settlements and vacant areas decreased by 20% and 38%. From 2010 to 2015, formal settlements, roads, vacant areas, and vegetation increased by 16%, 30%, 14%, and 17%, while informal settlements decreased by 4%. This indicates a greater focus by government authorities on planned development. From 2015 to 2020, formal settlements, roads, and vacant land increased by about 1.5%, 3%, and 14%, while informal settlements and vegetation decreased by 6% and 2%. The temporal and spatial TCA trajectory is shown in Fig. 6(a)–(c). The amount of settlement area designated as informal decreased, to be replaced by formal settlements. The magnitude of the change is low.

An object-based RF classification was used for the TSA model annual pattern definition. This flags a noticeable difference in the spectral characteristics of each class (Figs. 7 and 8). The

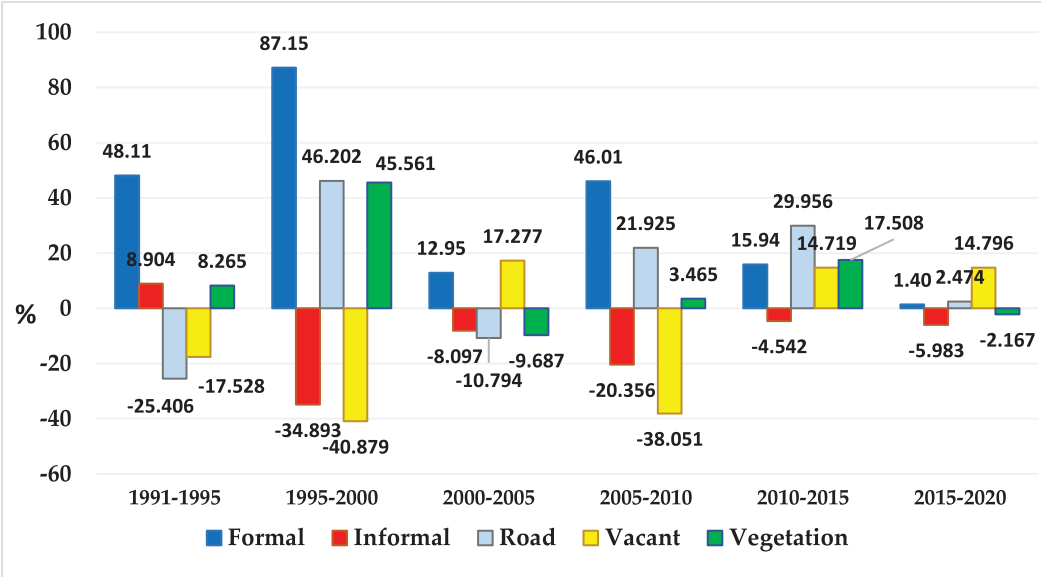

Fig. 5. Changes in land cover areas (%)—1991 to 2020.

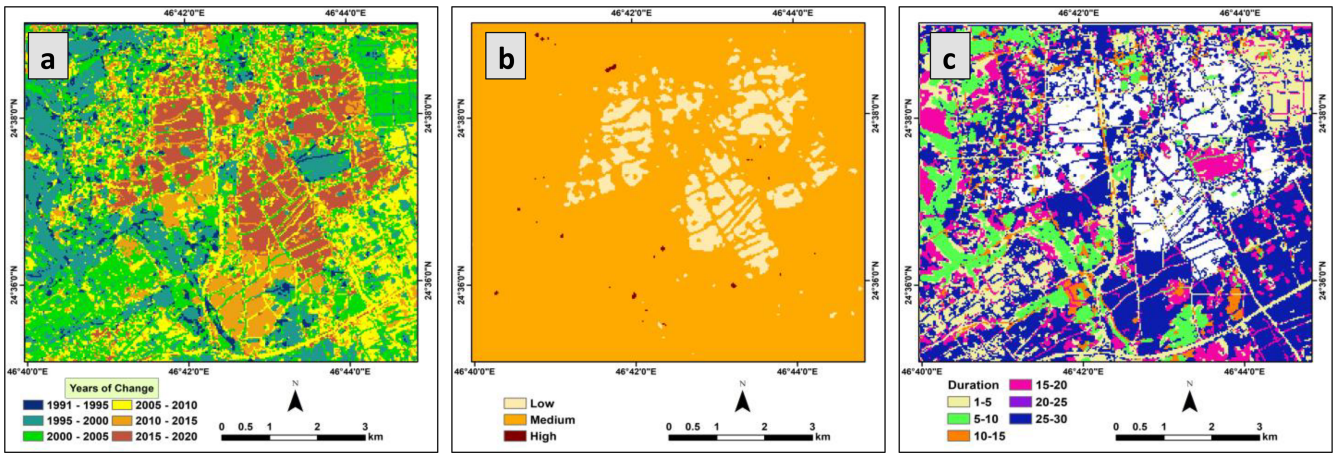

Fig. 6. Results of LandTrendr process: (a) is the years of change, (b) is magnitude, and (c) is the duration between 1991 and 2020.

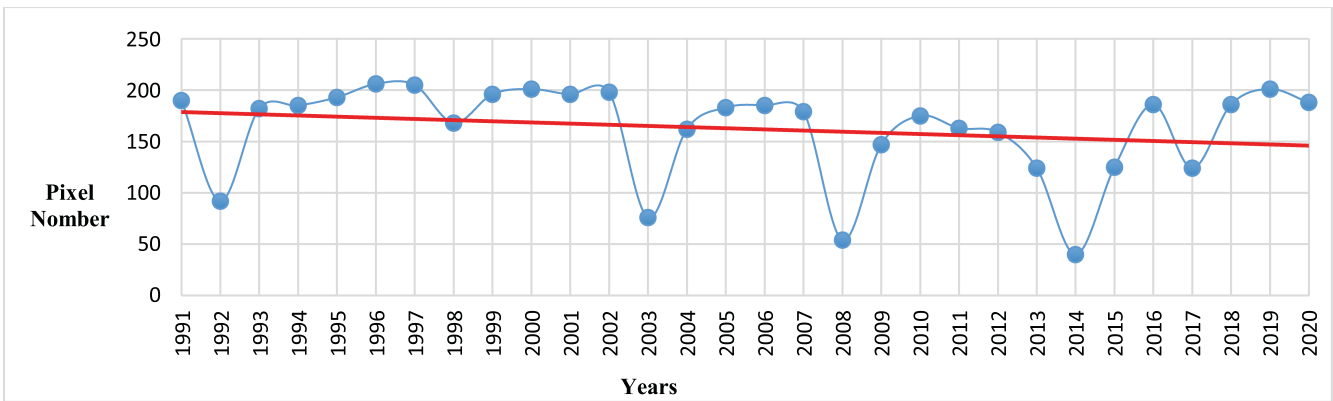

Fig. 7. Temporal TSA trendline trajectory of informal settlements.

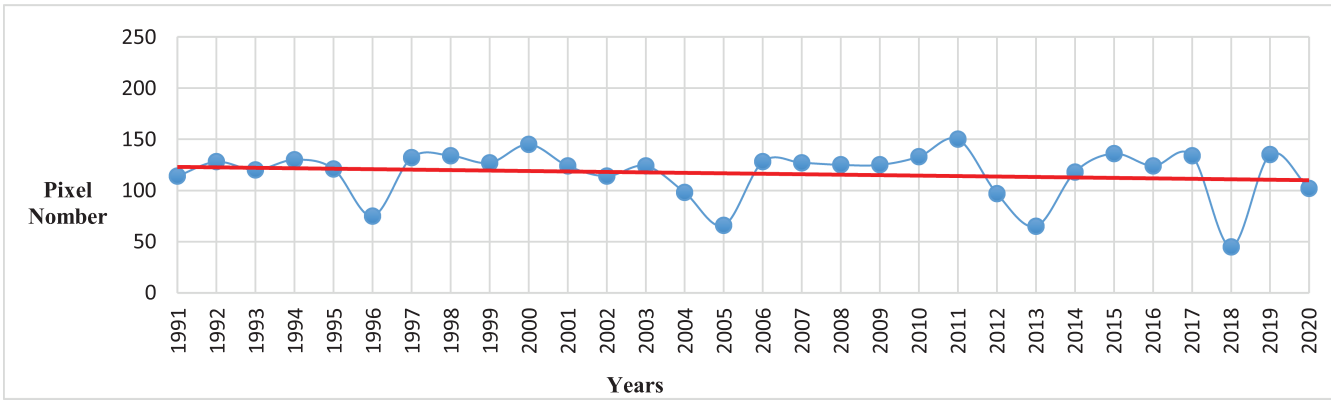

Fig. 8. Temporal TSA trendline trajectory of formal settlements.

TABLE IV
OVERALL ACCURACY OF THE OBIA–RF CLASSIFICATION—VHR IMAGERY WITH AND WITHOUT

ClassValue	Formal		Informal		Road		Vacant		Vegetation		Total		U Accuracy	
	With (TSA)	Without (TSA)	With (TSA)	Without (TSA)	With (TSA)	Without (TSA)	With (TSA)	Without (TSA)	With (TSA)	Without (TSA)	With (TSA)	Without (TSA)	With (TSA)	Without (TSA)
Formal	365	367	2	3	29	12	4	2	4	5	404	389	0.96	0.94
Informal	6	10	125	135	23	19	2	1	3	4	159	169	0.83	0.87
Road	4	4	2	1	532	520	1	0	0	0	539	525	0.97	0.94
Vacant	12	10	0	2	13	15	108	107	1	1	134	135	0.94	0.89
Vegetation	9	9	0	1	9	15	1	3	136	143	155	171	0.96	0.90
Total	396	400	129	142	606	581	116	113	144	153	1266	1266	0.00	0.00
PAccuracy	0.97	0.91	0.91	0.87	0.99	0.98	0.78	0.86	0.99	0.91	0	0		

Overall accuracy of OBIA-RF combined with (TSA) 89% and kappa 87%, and overall accuracy of OBIA-RF without combining (TSA) 87% and kappa 84%.

TABLE V
*F*1-SCORE OF THE OBIA–RF CLASSIFICATION

ClassValue	F1- score training		F1- score validation	
	With (TSA)	Without (TSA)	With (TSA)	Without (TSA)
Formal	0.93	0.91	0.92	0.88
Informal	0.86	0.86	0.87	0.86
Road	0.94	0.9	0.93	0.89
Vacant	0.89	0.88	0.89	0.85
Vegetation	0.92	0.91	0.89	0.87

distinguished changes appeared with the change of the trajectory trend in 30 years. The contribution was recorded according to the disturbance in spectral characteristics of each class. It can be observed that the changes of informal settlement areas were significantly transformed in 1992, 2003, 2008, and 2014 years (Fig. 7). The largest trajectory trend changes of formal settlements were significantly transformed in 1996, 2006, 2013, and 2018 years. These patterns were largely due to an increased focus by government on urban planning aimed at reducing the amount of informal settlements areas within the city boundaries (Fig. 8).

B. *Object-Based Ontology Indicators*

An assessment of the importance of the of the 30 indicators used within the classification is shown in Fig. 9. The OBIA–RF classification was evaluated using the three informal settlement

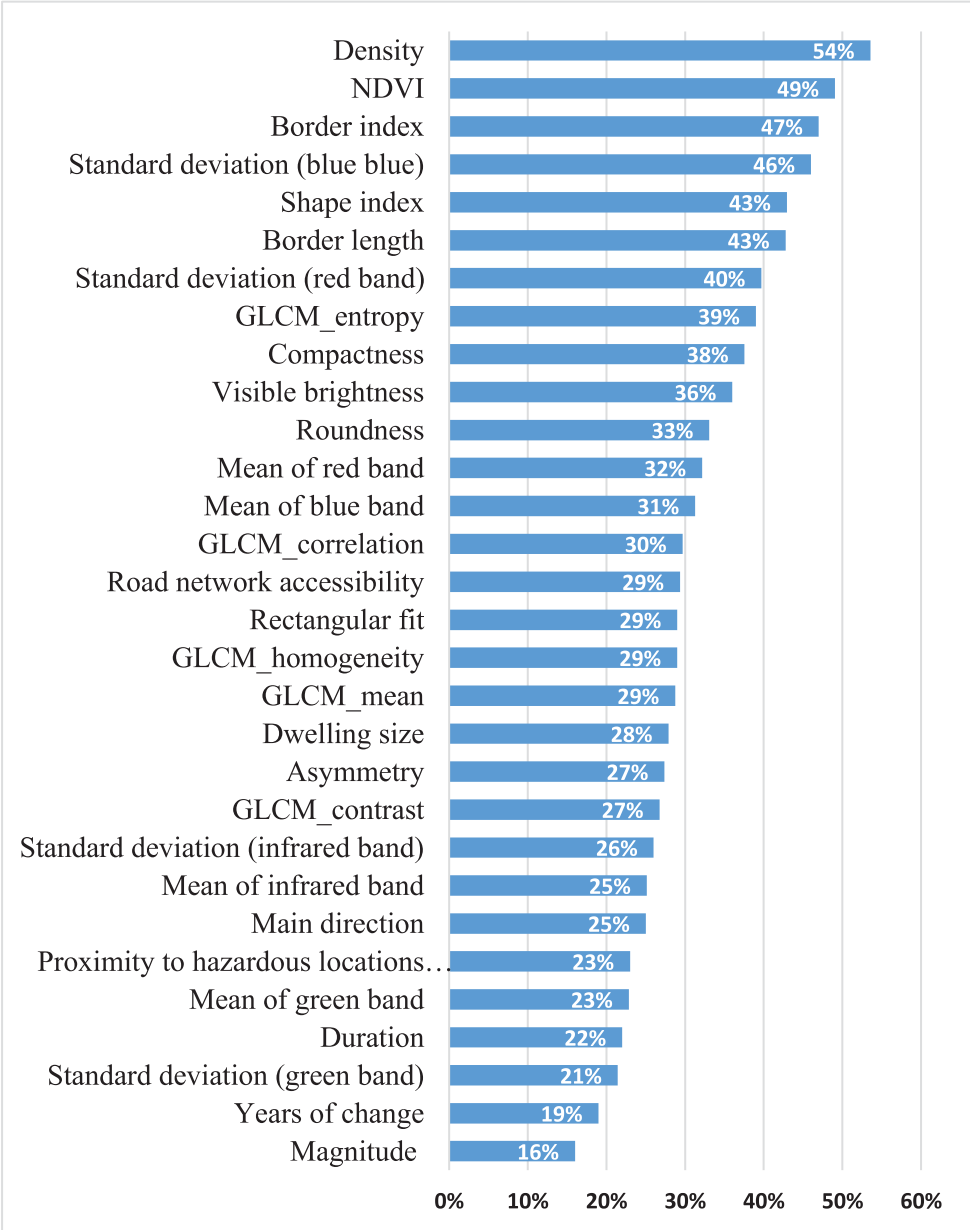

Fig. 9. OBIA–RF relative importance indicators.

spatial levels (object, settlement, and environ), as defined in the ontology.

At the object level, dwelling size was used to determine the characteristics of the object roof. OBIA–RF was employed to map dwelling size based on the characteristics of the buildings, including shape, size, and spacing. The dwelling size relative importance was identified as moderate (Fig. 9).

At the settlement level, density and NDVI were identified as the two most important indicators, with values of 54% and 49%, respectively. NDVI has been shown to greatly improve the accuracy of the classification process.

The third and fourth most important indicators, with values of 47% and 46%, thus demonstrating the importance of border index and standard deviation of blue (SDB) band in determining the shape of built-up areas, and therefore the ability to distinguish them from other classes. Shape index and border length were ranked as the fifth and sixth most important indicators, both with values of 43%, and are also considered important indicators.

The standard deviation of red (SDR) band was identified as the seventh most important indicator with a value of 40%. In contrast, the standard deviation of infrared band (SDIR) band was ranked 22nd with a value of 26%. This indicates that the SDB and SDR bands are more effective than the SDIR band for identifying informal and formal settlements when using OBIA–RF for the classification. The mean of the red band and mean of blue band were ranked as the 12th and 13th most important indicators, with values of 32% and 31%, respectively. The mean of the infrared band was ranked as the 23rd most important

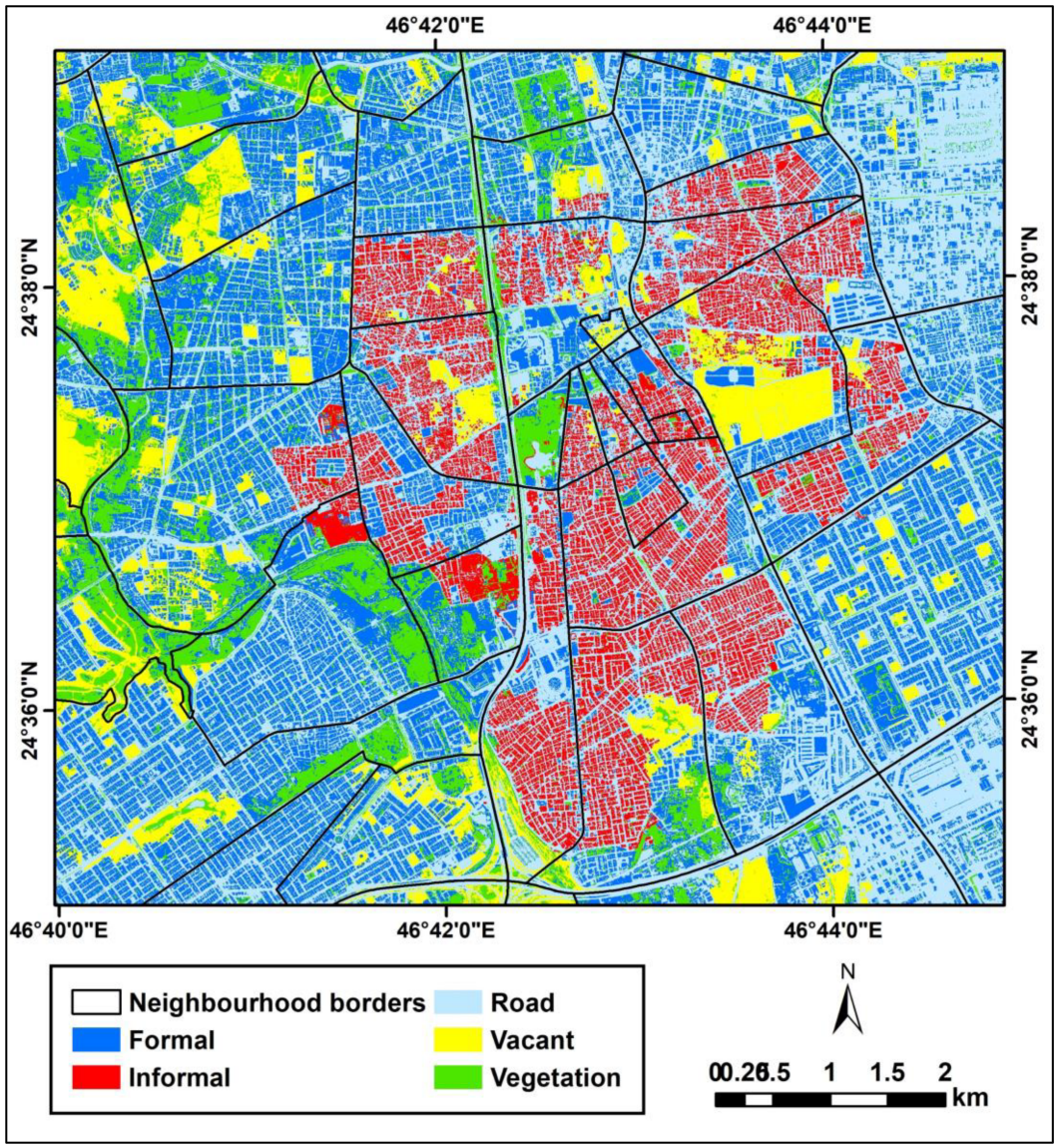

Fig. 10. Object-based ML RF classified Worldview-3 and Landsat imagery of informal and formal settlements in 2020 in Riyadh.

indicator with a value of 25%. This indicates the importance of using the visible bands in the OBIA–RF classification process and suggests that these bandwidths are particularly good for mapping informal settlements. The red and blue bands produce a higher reflectance value for buildings, vacant areas, and roads, than does infrared band (Fig. 9).

In urban areas, variables related to texture and structure are important. In this article, the GLCM was used to identify a descriptive vector for the texture of each segment. Five such measures were identified. GLCM entropy ranked foremost among the GLCM texture features, with a relative importance value of 39%. Four other GLCM textural features (correlation, homogeneity, mean, and contrast) were ranked as moderate indicators. Correlation recorded a value of 30%, while contrast returned a value of 27%. GLCM contrast appeared to have the least impact on image classification. GLCM contrast and homogeneity are inversely correlated: homogeneity decreases as contrast increases. Other textural measurements, such as variations in image segments or repetition defined by spectral intensity, are also very effective in identifying variations in informal settlement form.

The standard deviation of green band classification contribution was very small, as shown in Fig. 9. The standard deviation importance value of the blue band is also low. An improvement in classes was noted when the TSA descriptors were included. This can be observed as a slight improvement in the detection of the width of the road network and an increase in the road network connectivity. No improvement was noted in vacant land. In general, the indicators played a key role in the identification of informal settlements, however this was reduced in regards the TSA level variables. The three TSA level variables (duration, years of change, and magnitude) were ranked last.

Indicators at the environ level were less successful, consistently returning scores below those recorded at the settlement

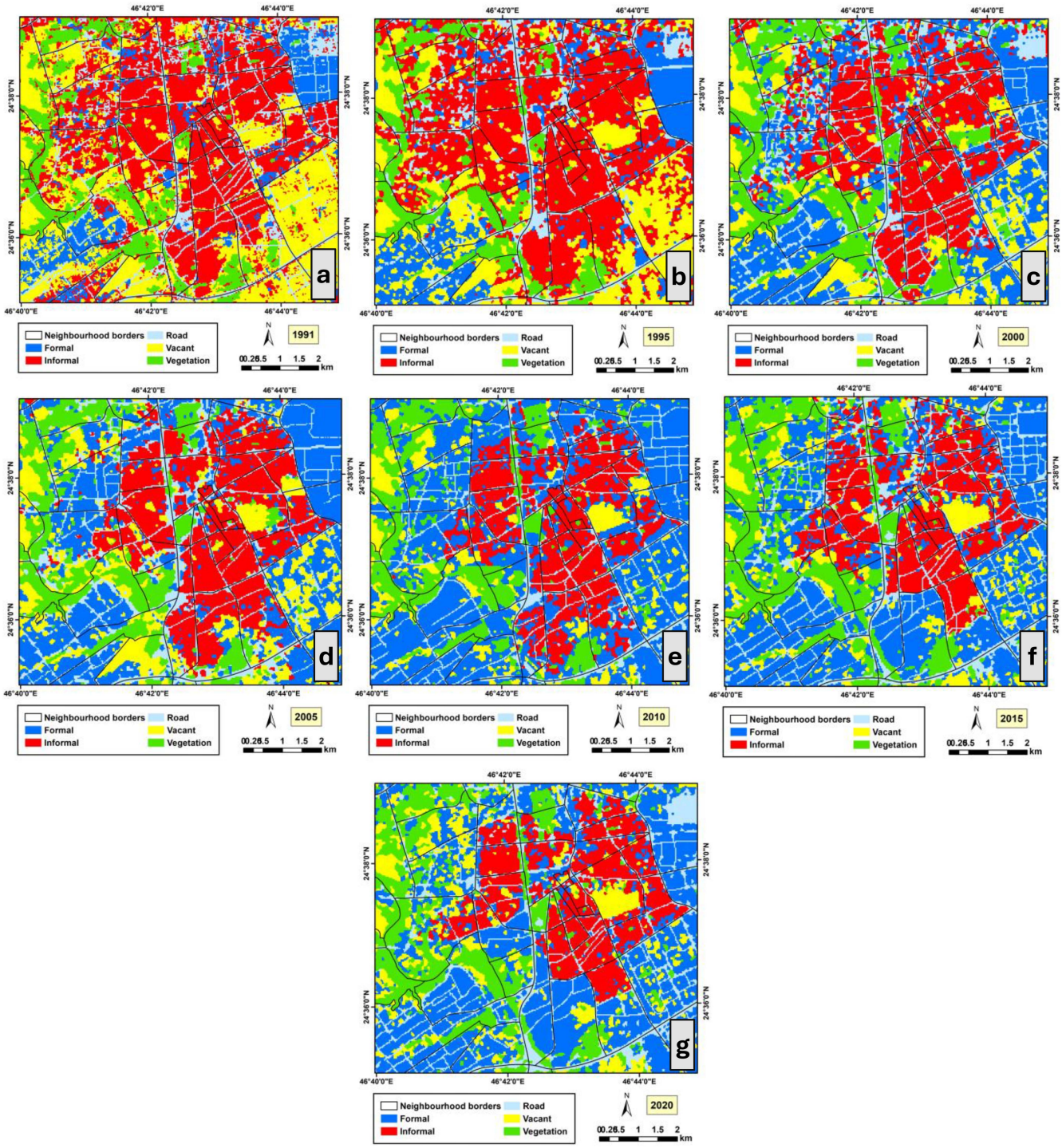

Fig. 11. Changes in informal settlements—1991 to 2020.

and object levels. The proximity to hazardous locations returned a very low value (23%). Slope and distance to potential hazards were determined using the DEM. Landslides and other potential hazards cannot occur due to the very flat terrain and so are disregarded as possible issues.

The analysis was conducted initially using TSA and then repeated without using TSA. Processing the data in this manner provides a good indication of the accuracy of each method. It appears from the results that any benefits derived by using the TSA method are lost due to the spectral similarity of objects within the study area. Clear and distinct spectral characteristics are required to successfully use this technique. The object-based ML (RF) classification using TSA is shown in Fig. 12(a), and without using TSA in Fig. 12(b). Processing the data using TSA, and including EK indicators and OBIA–RF, improves the accuracy of the final classification.

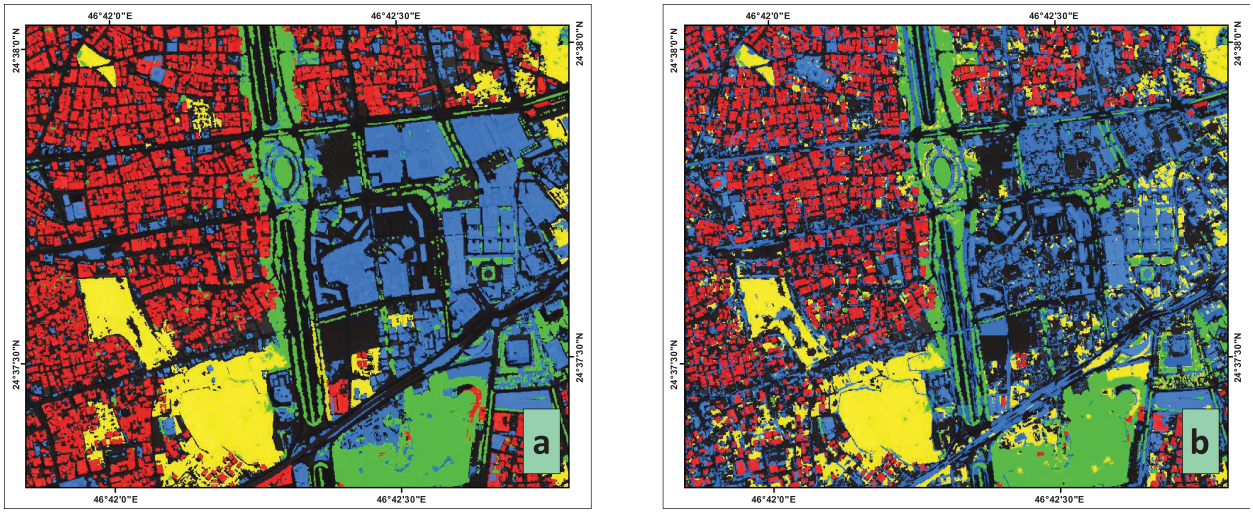

Fig. 12. Processing the data using TSA, including EK indicators and OBIA-RF, improves the accuracy of the final classifi cation. (a) Combined OBIA–RF with TSA and 12, (b) without combining OBIA–RF with TSA.

C. Accuracy Assessment

The results of accuracy assessment are shown in Tables IV and V. OA of the OBIA–RF classification combined with the VHR imagery and TSA variables was 89%. The kappa was 87%. When removing the TSA variables, the accuracy was 87% and kappa was 84%. This shows that there is a definite improvement in classification when using the TSA variables (Fig. 5).

IV. Discussion

The $F1$-score accuracy is shown in Table V. The four classes (formal, road, vacant, and vegetation) returned a higher user accuracy $F1$-score using the TSA variables, than when they were processed without using the TSA variables. The results indicate very good informal settlement identification ability. The current article evaluated an ontology originally developed by Alrasheedi et al. [9] for mapping informal settlements in Riyadh city, KSA, and introduced an expanded dataset. The article incorporated 30 years of Landsat and Worldview-3 imagery, TSA techniques, and local EK. Twenty-eight neighborhoods were examined, with thirty urban indicators used in the analysis. These were categorized into five main classes—informal and formal settlements, vacant areas, road networks, and vegetation.

OBIA–RF, an ML technique, was employed in the data processing. The spectral characteristics from high-resolution WorldView-3 was integrated with segmented Landsat imagery and used to assess the validity of using these techniques for mapping informal settlements. Landtrendr and TSA—two contrasting change detection methods—were used to identify the temporal and spatial dynamics found within informal settlement areas. These were combined with OBIA–RF to classify the data. The accuracy of the final classification was then assessed using a confusion matrix and $F1$ score.

The article used TSA (represented by a multidimensional cube) and LandTrendr to identify spatiotemporal changes noticeable in the Landsat images. OBIA was used in the segmentation stage to generate unique indicators for the processing phase, as recommended by local experts. These indicators served as input data for the classification of the Worldview-3 imagery, resulting in improved model performance and increased accuracy for each of the predicted classes (Table III). This underscores the crucial role that a combination of Landsat and VHR images can play in effectively mapping urban development as previously highlighted by [37]. The classification results confirm the suitability of this integrated approach.

A small improvement in accuracy was obtained when including TSA in the classification process (Table IV). The OBIA–RF classification recorded an accuracy score of 89% and a Kappa of 87%. The smallest contribution to the ontology was made by using TSA, in combination with LandTrendr and OBIA, as input data. LandTrendr is a pixel-based algorithm, so the results needed to be generalized to integrate it with the segments generated from the Landsat and VHR imagery.

Riyadh's informal settlements are commonly located within the old skirt, in contrast to the usual situation where they are usually situated outside the city centers [38], [39], [40]. Parts of the old city contain historical buildings with significant heritage value. The location of these structures has been designated restricted areas by the government and programs to upgrade and refine them have been underway for some time. Structures in other parts of the informal settlements, however, have been erected without conformance to any regulatory planning or engineering requirements, or adherence to the Saudi Building Code (SBC) [41], [42]. The SBC defines various technical, regulatory, and legal requirements (as well as administrative guidelines) that establish minimum standards for building construction, and ensure public health and safety standards are met [41], [42]. This planning and development process differs from other countries where urban redevelopment normally leads to the displacement of residents from informal settlements. This typically renders them homeless due to the high cost of housing and the lack of any financial support from the government [43], [44]. In the KSA, the fundamental components of the development process encompass the delivery of public services, residential

construction development, urban planning, and the rehabilitation of affected areas, all with comprehensive government assistance [45]. This article supports the idea that using multitemporal data imagery has the potential to provide suitable inputs for simulation modeling which can enable the efficient and accurate analysis of informal settlement expansion. This is promising in regards providing policy-relevant insights into future development scenarios [13], [46], [47], [48], [49], [50].

The article incorporated GLCM texture-based analysis to capture urban morphological features. The density of built-up areas was ranked as the most important indicator in regards shape, size, orientation, and roof material type. This approach involves defining five GLCM measures (used to identify a vector) by describing the texture of each segment and has been undertaken in previous article [8], [9]. These measures were integrated into the current article. An improved ability to identify morphological attributes within informal settlements was achieved and it appears that the integration of various texture descriptors is essential for effectively distinguishing between these complex urban settlement patterns. This aligns with the findings of prior articles [35], [51]. OBIA–RF, in conjunction with local expert opinions, shows a very good ability to capture the morphological characteristics of informal settlements compared to temporal analysis studies that rely solely on ML or OBIA. The OBIA–RF classification revealed that GLCM entropy is the best GLCM indicator to use for distinguishing between buildings in formal and informal built-up areas. It is therefore suggested that the GLCM entropy variable is included in any future change detection studies, particularly when employing TSA. The incorporation of texture into ML methods was found to be effective and contributed to the enhancement of classification accuracy, especially when applied to the VHR imagery.

One issue identified in regards discriminating between informal and formal settlements relates to the spectral mixing occurring between roof buildings and vacant areas, and hence difficulty in separating these differing features. This is attributed to winds depositing sand onto building roofs and hence providing a similar spectral response pattern when viewed in the satellite imagery. This finding agrees with previous articles [52], [53], [54]. The use of blue, red, and NIR band standard deviation values also appears to be an effective classification tool. This observation aligns with the findings of prior articles by Alrasheedi et al. [9] and Rouibah [55]. These findings indicate that the blue band is effective in identifying built-up areas and road networks, the red band is useful in GLCM processing for discerning building textures, and the NIR band can be used for effectively recognizing features, such as vegetation and vacant areas [8], [35]. The standard deviation of the green band, on the other hand, appears to be less effective in the OBIA–RF settlement classification work. The use of the mean of the blue, red, and infrared bands provided only moderate ranking values and proved less effective than the use of standard deviation values. This article confirms that using the band standard deviation of VHR images is superior to using the band mean of these images when applying ML techniques in classification work. The results show that using area-relevant indicators as inputs produces superior outcomes in regards informal settlement identification. Despite increasing the feature space dimensionality as a result of adding additional features, such as textural variables to the spectral bands, the article suggests that incorporating more input variables could actually improve the ability to distinguish between settlement types. This aligns with the observation noted in a previous article that extracting a large number of relevant features from satellite data can actually enhance image classification accuracy as [56].

The current article drawn upon the ontological framework developed by Alrasheedi et al. [9] for mapping settlement areas in the Arabian Peninsula. It confirmed the effectiveness of ontology-based temporal analysis in defining the characteristics of these built-up areas. It also incorporates the use of EK about the actual study areas. This enables identification of indicators unique to these areas which are regarded as of significant value for the processing phase. A further benefit of this article relates to the transferability of the concepts across diverse geographical locations.

V. Conclusion

This article assessed the transferability potential of the original informal settlement ontology developed by Alrasheedi et al. [8] and [9]. It utilized new datasets and introduced new spatial–temporal analysis methods as part of the assessment work. The ontology was designed to integrate OBIA and ML (RF) methods using Worldview-3 and Landsat imagery as inputs. It also utilized remote-sensing-based TSA detection methods and 30 EK indicators to define all spatiotemporal changes evident in selected areas of the Riyadh city between 1991 and 2020. Three key study objectives were successfully achieved.

1) The accurate identification and mapping of the informal settlement areas.
2) Differentiation of informal from formal settlements using an OBIA–RF classification process.
3) Detection of informal settlement spatiotemporal changes over a period of 30 years using a TSA method.

An advantage of the techniques assessed lies in the effortless incorporation of OBIA and ML (RF) into the existing ontological framework. The purpose of this combination is to simplify and improve the readability of the classification process in regards remotely sensed data.

The utilization of the ML (RF) method effectively addresses some challenges presented by OBIA, such as issues regarding accuracy, and the efficient handling of large datasets. The selected OBIA–RF approach also demonstrated the effectiveness of each indicator in the settlement identification process. The informal settlement mapping results provided an OA combined with (TSA) of 89% and Kappa of 87%, and OA of OBIA–RF without combining (TSA) of 87% and Kappa of 84%. Based on the results, indicators at the settlement level appear to have the most influence on informal settlements mapping.

Certain limitations were noted. The green band was ranked as a weak indicator. This should be investigated in more detail in any future articles. Informal settlement mapping work should also utilize three-dimensional (3-D) and multispectral data (potentially acquired using drones) to construct 3-D models from

orthophotos. By employing these methods, a reliable dataset suitable for more detailed informal settlement mapping can be developed. This article has shown that the use of object-oriented analysis techniques should be encouraged, with a future focus on the capabilities evident in Google Earth Engine.

The analysis of TSA provides valuable insights into the spatial and temporal dynamics of informal settlements in Arabian Peninsula. This aids in the understanding of long-term trends and introduce a future sight informing future urban planning strategies. The article provides a useful tool for urban planners and policymakers to identify and manage informal settlements, which can help with infrastructure design and implementation, as well as environmental, social, and financial impact assessments.

ACKNOWLEDGMENT

Khlood Ghalibr Alrasheedi expresses gratitude to the Ministry of Education in the Kingdom of Saudi Arabia for the doctoral scholarship initiative. Appreciation is also extended to the King Abdulaziz City for Science and Technology for supplying the WordView-3 imagery essential for this article. Heartfelt thanks are extended to all the experts who actively participated in the survey, generously sharing their valuable experience and knowledge. The support from the Municipality and the Royal Commission for Riyadh City is acknowledged and greatly appreciated.

REFERENCES

[1] A. Abascal et al., "Domains of deprivation framework" for mapping slums, informal settlements, and other deprived areas in LMICs to improve urban planning and policy: A scoping review," *Comput., Environ. Urban Syst.*, vol. 93, 2022, Art. no. 101770.

[2] A. P. Salinger et al., "People are now working together for a common good": The effect on social capital of participatory design for community-level sanitation infrastructure in urban informal settlements," *World Develop.*, vol. 174, 2024, Art. no. 106449.

[3] H. Kekana, T. Ruhiiga, N. Ndou, and L. Palamuleni, "Environmental justice in South Africa: The dilemma of informal settlement residents," *GeoJournal*, vol. 88, pp. 3709–3725, 2023.

[4] Y. Adewunmi, U. E. Chigbu, S. Mwando, and U. Kahireke, "Entrepreneurship role in the co-production of public services in informal settlements—A scoping review," *Land Use Policy*, vol. 125, 2023, Art. no. 106479.

[5] A. M. Dewan and Y. Yamaguchi, "Effect of land cover changes on flooding: Example from Greater Dhaka of Bangladesh," *Int. J. Geoinform.*, vol. 4, no. 1, pp. 11–20, 2008.

[6] M. Kuffer, K. Pfeffer, and R. Sliuzas, "Slums from space—15 years of slum mapping using remote sensing," *Remote Sens.*, vol. 8, no. 6, 2016, Art. no. 455.

[7] N. Mudau and P. Mhangara, "Mapping and assessment of housing informality using object-based image analysis: A review," *Urban Sci.*, vol. 7, no. 3, 2023, Art. no. 98.

[8] K. G. Alrasheedi, A. Dewan, and A. El-Mowafy, "Mapping informal settlements using machine learning techniques, object-based image analysis and local knowledge," in *Proc. IEEE Int. Geosci. Remote Sens. Symp.*, 2023, pp. 7249–7252.

[9] K. G. Alrasheedi, A. Dewan, and A. El-Mowafy, "Using local knowledge and remote sensing in the identification of informal settlements in Riyadh City, Saudi Arabia," *Remote Sens.*, vol. 15, no. 15, 2023, Art. no. 3895.

[10] P. Hofmann, J. Strobl, T. Blaschke, and H. Kux, "Detecting informal settlements from QuickBird data in Rio de Janeiro using an object based approach," in *Object-Based Image Analysis*. Berlin, Germany: Springer, 2008, pp. 531–553.

[11] D. Kohli, R. Sliuzas, and A. Stein, "Urban slum detection using texture and spatial metrics derived from satellite imagery," *J. Spatial Sci.*, vol. 61, no. 2, pp. 405–426, 2016.

[12] N. Mboga, C. Persello, J. R. Bergado, and A. Stein, "Detection of informal settlements from VHR images using convolutional neural networks," *Remote Sens.*, vol. 9, no. 11, 2017, Art. no. 1106.

[13] H. Park, P. Fan, R. John, Z. Ouyang, and J. Chen, "Spatiotemporal changes of informal settlements: Ger districts in Ulaanbaatar, Mongolia," *Landscape Urban Plan.*, vol. 191, 2019, Art. no. 103630.

[14] P. Hofmann, H. Taubenböck, and C. Werthmann, "Monitoring and modelling of informal settlements-A review on recent developments and challenges," in *Proc. Joint Urban Remote Sens. Event*, 2015, pp. 1–4.

[15] O. Kit, M. Lüdeke, and D. Reckien, "Texture-based identification of urban slums in Hyderabad, India using remote sensing data," *Appl. Geogr.*, vol. 32, no. 2, pp. 660–667, 2012.

[16] M. S. Abebe, K. T. Derebew, and D. O. Gemeda, "Exploiting temporal-spatial patterns of informal settlements using GIS and remote sensing technique: A case study of Jimma city, Southwestern Ethiopia," *Environ. Syst. Res.*, vol. 8, no. 1, pp. 1–11, 2019.

[17] K. Musungu and Z. T. Mkhize, "Change detection in the horticultural region of Cape Town using Landsat imagery," in *Proc. Earth Observ. Geospatial Sci. Service Sustain. Develop. Goals: 12th Int. Conf. Afr. Assoc. Remote Sens. Environ.*, 2019, pp. 69–76.

[18] J. Pratomo, M. Kuffer, D. Kohli, and J. Martinez, "Application of the trajectory error matrix for assessing the temporal transferability of OBIA for slum detection," *Eur. J. Remote Sens.*, vol. 51, no. 1, pp. 838–849, 2018.

[19] L. Yang, K. Cormican, and M. Yu, "Ontology-based systems engineering: A state-of-the-art review," *Comput. Ind.*, vol. 111, pp. 148–171, 2019.

[20] D. Matarira, O. Mutanga, M. Naidu, and M. Vizzari, "Object-based informal settlement mapping in Google Earth Engine using the integration of Sentinel-1, Sentinel-2, and PlanetScope satellite data," *Land*, vol. 12, no. 1, 2022, Art. no. 99.

[21] O. Kit and M. Lüdeke, "Automated detection of slum area change in Hyderabad, India using multitemporal satellite imagery," *ISPRS J. Photogrammetry Remote Sens.*, vol. 83, pp. 130–137, 2013.

[22] J. H. Breuer and J. Friesen, "Methods to assess spatio-temporal changes of slum populations," *Cities*, vol. 143, 2023, Art. no. 104582.

[23] M. Kuffer et al., "Spatial information gaps on deprived urban areas (slums) in low-and-middle-income-countries: A user-centered approach," *Urban Sci.*, vol. 5, no. 4, 2021, Art. no. 72.

[24] K. Dovey, M. van Oostrum, I. Chatterjee, and T. Shafique, "Towards a morphogenesis of informal settlements," *Habitat Int.*, vol. 104, 2020, Art. no. 102240.

[25] J. Carrilho and J. Trindade, "Sustainability in peri-urban informal settlements: A review," *Sustainability*, vol. 14, no. 13, 2022, Art. no. 7591.

[26] R. Prabhu and R. A. Raja, "Urban slum detection approaches from high-resolution satellite data using statistical and spectral based approaches," *J. Indian Soc. Remote Sens.*, vol. 46, no. 12, pp. 2033–2044, 2018.

[27] R. Prabhu, B. Parvathavarthini, and R. A. Raja, "Slum extraction from high resolution satellite data using mathematical morphology based approach," *Int. J. Remote Sens.*, vol. 42, no. 1, pp. 172–190, 2021.

[28] S. K. Hanoon, A. F. Abdullah, H. Z. Shafri, and A. Wayayok, "Comprehensive vulnerability assessment of urban areas using an integration of fuzzy logic functions: Case study of Nasiriyah City in South Iraq," *Earth*, vol. 3, no. 2, pp. 699–732, 2022.

[29] N. L. Maung, A. Kawasaki, and S. Amrith, "Spatial and temporal impacts on socio-economic conditions in the Yangon slums," *Habitat Int.*, vol. 134, 2023, Art. no. 102768.

[30] Q. Feng, J. Liu, and J. Gong, "UAV remote sensing for urban vegetation mapping using random forest and texture analysis," *Remote Sens.*, vol. 7, no. 1, pp. 1074–1094, 2015.

[31] G. Leonita, M. Kuffer, R. Sliuzas, and C. Persello, "Machine learning-based slum mapping in support of slum upgrading programs: The case of Bandung City, Indonesia," *Remote Sens.*, vol. 10, no. 10, 2018, Art. no. 1522.

[32] P. Fu and Q. Weng, "A time series analysis of urbanization induced land use and land cover change and its impact on land surface temperature with Landsat imagery," *Remote Sens. Environ.*, vol. 175, pp. 205–214, 2016.

[33] M. Kuffer, K. Pfeffer, R. Sliuzas, and I. Baud, "Extraction of slum areas from VHR imagery using GLCM variance," *IEEE J. Sel. Topics Appl. Earth Observ. Remote Sens.*, vol. 9, no. 5, pp. 1830–1840, May 2016.

[34] R. Khraif, A. A. Salam, J. Al-Ayeen, and M. F. Abdul, "Residential satisfaction in shantytowns of Riyadh City, Saudi Arabia: Levels and determinants," *Glob. J. Res. Rev.*, vol. 5, no. 3, pp. 12–20, 2018.

[35] D. Matarira, O. Mutanga, and M. Naidu, "Google Earth Engine for informal settlement mapping: A random forest classification using spectral and textural information," *Remote Sens.*, vol. 14, no. 20, 2022, Art. no. 5130.

[36] B. Ghimire, J. Rogan, V. R. Galiano, P. Panday, and N. Neeti, "An evaluation of bagging, boosting, and random forests for land-cover classification in Cape Cod, Massachusetts, USA," *GISci. Remote Sens.*, vol. 49, no. 5, pp. 623–643, 2012.

[37] T. Lu, D. Ming, X. Lin, Z. Hong, X. Bai, and J. Fang, "Detecting building edges from high spatial resolution remote sensing imagery using richer convolution features network," *Remote Sens.*, vol. 10, no. 9, 2018, Art. no. 1496.

[38] J. C. Duque, J. E. Patino, and A. Betancourt, "Exploring the potential of machine learning for automatic slum identification from VHR imagery," *Remote Sens.*, vol. 9, no. 9, 2017, Art. no. 895.

[39] J. Li, X. Huang, L. Tu, T. Zhang, and L. Wang, "A review of building detection from very high resolution optical remote sensing images," *GISci. Remote Sens.*, vol. 59, no. 1, pp. 1199–1225, 2022.

[40] R. Mahabir, P. Agouris, A. Stefanidis, A. Croitoru, and A. T. Crooks, "Detecting and mapping slums using open data: A case study in Kenya," *Int. J. Digit. Earth*, vol. 13, no. 6, pp. 683–707, 2020.

[41] A. Shamseldin, "Proposed role of the local Saudi building codes in assessing the energy performance of buildings in KSA's GBRS," *Ain Shams Eng. J.*, vol. 14, no. 5, 2023, Art. no. 101966.

[42] M. S. Alghamdi, T. H. Beach, and Y. Rezgui, "Reviewing the effects of deploying building information modelling (BIM) on the adoption of sustainable design in Gulf countries: A case study in Saudi Arabia," *City, Territory Architecture*, vol. 9, no. 1, pp. 1–17, 2022.

[43] S. Patel, R. Sliuzas, and N. Mathur, "The risk of impoverishment in urban development-induced displacement and resettlement in Ahmedabad," *Environ. Urbanization*, vol. 27, no. 1, pp. 231–256, 2015.

[44] D. Stow, A. Lopez, C. Lippitt, S. Hinton, and J. Weeks, "Object-based classification of residential land use within Accra, Ghana based on QuickBird satellite data," *Int. J. Remote Sens.*, vol. 28, no. 22, pp. 5167–5173, 2007.

[45] A. M. Ajlan and A. M. Al Abed, "Transformation model towards sustainable smart cities: Riyadh, Saudi Arabia as a case study," *Curr. Urban Stud.*, vol. 11, no. 1, pp. 142–178, 2023.

[46] D. Jovanović, M. Gavrilović, D. Sladić, A. Radulović, and M. Govedarica, "Building change detection method to support register of identified changes on buildings," *Remote Sens.*, vol. 13, no. 16, 2021, Art. no. 3150.

[47] M. Hussain, D. Chen, A. Cheng, H. Wei, and D. Stanley, "Change detection from remotely sensed images: From pixel-based to object-based approaches," *ISPRS J. Photogrammetry Remote Sens.*, vol. 80, pp. 91–106, 2013.

[48] A. M. Dewan and Y. Yamaguchi, "Land use and land cover change in Greater Dhaka, Bangladesh: Using remote sensing to promote sustainable urbanization," *Appl. Geogr.*, vol. 29, no. 3, pp. 390–401, 2009.

[49] L. Okore, J. Koske, and S. Letema, "Scenarios for adoption of low-carbon household cooking fuels in biomass-dependent informal settlements of urban Sub-Saharan Africa: A critical analysis of Kisumu City," *East Afr. J. Environ. Natural Resour.*, vol. 7, no. 1, pp. 28–48, 2024.

[50] V. K. Singh and V. Kumar, "Enhancing emergency vehicle access in dense settlements of Mumbai using high-resolution satellite imagery: A deep learning approach," *Int. J. Disaster Risk Reduction*, vol. 100, 2024, Art. no. 104212.

[51] J. Graesser, A. Cheriyadat, R. R. Vatsavai, V. Chandola, J. Long, and E. Bright, "Image based characterization of formal and informal neighborhoods in an urban landscape," *IEEE J. Sel. Topics Appl. Earth Observ. Remote Sens.*, vol. 5, no. 4, pp. 1164–1176, Aug. 2012.

[52] J. Chen, P. Du, C. Wu, J. Xia, and J. Chanussot, "Mapping urban land cover of a large area using multiple sensors multiple features," *Remote Sens.*, vol. 10, no. 6, 2018, Art. no. 872.

[53] B.-E. Dolean et al., "Evaluation of the built-up area dynamics in the first ring of Cluj-Napoca metropolitan area, Romania by semi-automatic GIS analysis of Landsat satellite images," *Appl. Sci.*, vol. 10, no. 21, 2020, Art. no. 7722.

[54] H. A. Zurqani, C. J. Post, E. A. Mikhailova, and J. S. Allen, "Mapping urbanization trends in a forested landscape using Google Earth Engine," *Remote Sens. Earth Syst. Sci.*, vol. 2, pp. 173–182, 2019.

[55] K. Rouibah, "The use of bands ratio derived from Sentinel-2 imagery to detect built-up area in the dry period (North-East Algeria)," *Appl. Geomatics*, vol. 15, pp. 473–482, 2023.

[56] F. Mohseni, M. Amani, P. Mohammadpour, M. Kakooei, S. Jin, and A. Moghimi, "Wetland mapping in great lakes using sentinel-1/2 time-series imagery and DEM data in Google Earth Engine," *Remote Sens.*, vol. 15, no. 14, 2023, Art. no. 3495.

Khlood Ghalibr Alrasheedi (Fellow, IEEE), photograph and biography not available at the time of publication.

Ashraf Dewan, photograph and biography not available at the time of publication.

Ahmed El-Mowafy (Member, IEEE), photograph and biography not available at the time of publication.